PHYSICAL REVIEW B VOLUME 41, NUMBER 11 15 APRIL 1990-I

Electrostatic electron lens in the ballistic regime

U. Sivan, M. Heiblum, C. P. Umbach, and H. Shtrikman
IBM Research Division, Thomas J. Watson Research Center, Yorktown Heights, New York 10598
(Received 16 January 1990)

Electrostatic focusing of ballistic electrons in a high-mobility two-dimensional electron gas is discussed and experimentally demonstrated. The focusing is achieved by a spatial modulation of the electrostatic potential along the electrons' trajectories, in analogy with the modulation of the dielectric constant in conventional light-wave optics.

The long electronic mean free path (mfp) in two-dimensional electron-gas (2D EG) systems and improved electron-beam lithography have opened a new field of research which might be called "electron optics in solids." A few recent examples are magnetic focusing,[1] the collimation of an electron beam injected from a smooth constriction,[2-4] electrostatic beam steering,[3] and Fabry-Pérot modes in a 1D electron resonator.[5,6] All of these effects involve reflective elements, namely scattering off potentials higher than the electron energy. It is the purpose of this paper to report on the first realization of a purely refractive element, namely an electrostatic electron lens. The electronic imaging described below is obtained by spatial modulation of the electrostatic potential in the space where ballistic electrons travel, in analogy with the spatial modulation of the dielectric constant in standard optical lenses.

The corresponding "Snell's law" for ballistic electrons that cross a boundary where their velocity is changed can be derived from the classical equations of motion. Consider the case depicted in Fig. 1(a) where an electron at the Fermi energy E_F impinges at an angle θ_1 on an interface between two regions with different carrier concentration, $N_1 = mE_F/\pi\hbar^2$ and $N_2 = m(E_F - \Phi)/\pi\hbar^2$, respectively. Since the momentum parallel to the interface is conserved, $p_1 \sin\theta_1 = p_2 \sin\theta_2$ (where p_1, p_2 are the total electron momenta in the two regions); energy conservation yields

$$\sin\theta_1/\sin\theta_2 = (1 - \Phi/E_F)^{1/2}, \quad (1)$$

which is the analog of Snell's law. Notice that for positive Φ, θ_2 is larger than θ_1, in contrast with the case of a photon entering a medium with a larger dielectric constant. This difference results from the different dispersion relations for massive particles and photons. In the first case, lower velocity is accompanied by longer wavelength while in the case of photons a larger index of refraction leads to a lower velocity and a shorter wavelength. In the experiment described below, Φ is positive and a converging lens has a concave shape.

The lens device was fabricated on a GaAs-$Al_xGa_{1-x}As$ heterojunction supporting a high-mobility 2D EG. The carrier density and mobility of the 2D EG were measured at 4.2 K using a standard van der Pauw procedure and were found to be $N_S \simeq 3\times10^{11}$ cm^{-2} and $\mu \simeq 7\times10^5$ cm^2/V sec, respectively, leading to a Fermi energy $E_F = 10.7$ meV and a transport mfp (calculated from the mobility) of $l \simeq 4.5$ μm. A scanning electron micrograph of a typical device is shown in Fig. 2. Two metallic gates define a point emitter (E) while four other gates arranged along a circumference of a circle define three voltage probes ($P1$ to $P3$) at angles of $-30°$, $0°$, and $30°$ relative to the emitter axis. The nominal sizes of the emitter and probes openings varied between 180 and 500 nm and the radius of the device was usually 2.2 μm (we have fabricated larger devices as well as will be mentioned below). A biconcave shaped gate in the center of the structure served as a lens gate with two circular faces having radius $R = 400$ nm and "waist width" $W = 400$ nm. The microstructure was defined using electron-beam lithography. The emitter (E), the three probes ($P1$, $P2$, $P3$), and the two drain contacts ($D1$, $D2$) were contacted using standard Ni-Ge-Au alloyed ohmic contacts. Application of a high enough negative bias to the emitter and the probes gates created potential barriers, higher than E_F, underneath these gates, which confined the electrons to the

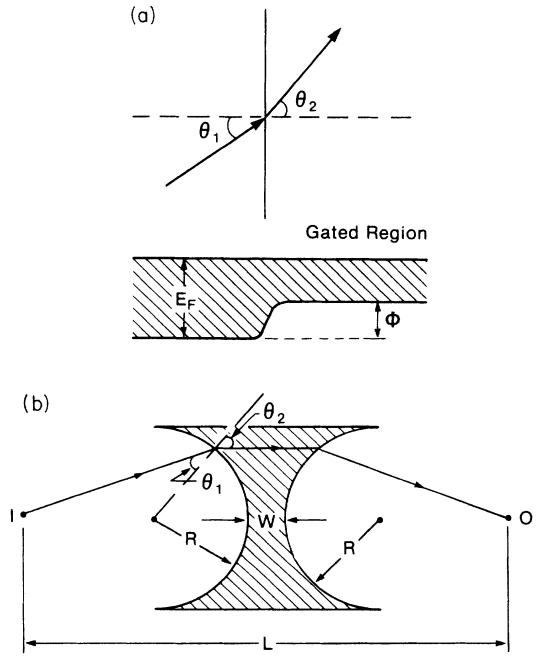

FIG. 1. (a) The geometry assumed in the derivation of Snell's law. (b) Schematics of the biconcave lens leading to Eq. (2) for the imaging conditions.

 © 1990 The American Physical Society

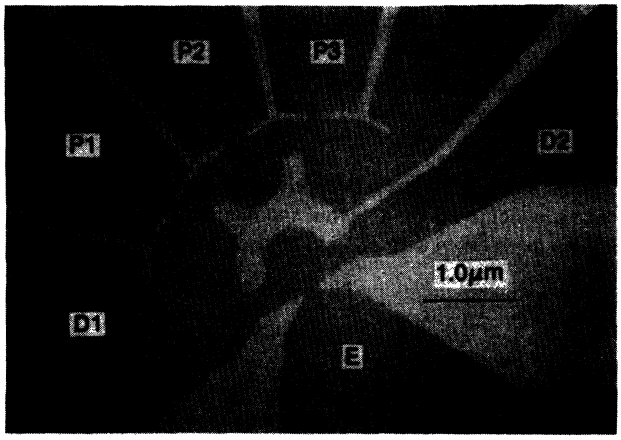

FIG. 2. Scanning electron microscope micrograph of the device (top view). The light areas are the metallic gates forming the emitter, probes, and the biconcave lens, by the induction of potential barriers underneath.

ungated and the lens regions. Application of a small negative bias to the lens gate formed a shallow potential barrier under the gate with a spatial shape similar to that of the lens. The potential Φ formed under the lens gate depended on the applied voltage V_{GL} and could be tuned between zero and values larger than E_F. The ratio $\sin\theta_2/\sin\theta_1$ [Fig. 1(a)] could thus be varied between unity and infinity, changing the focal length of the lens between the lens radius and infinity. The distance L between an object (O) and its image (I), assuming the lens is equidistant to O and I [Fig. 1(b)], can be calculated using Eq. (1). For small θ_1, θ_2 it is given by

$$L=\frac{2R}{1-(1-\Phi/E_F)^{1/2}}+W, \tag{2}$$

which for the device depicted in Fig. 2 with $L=2.2$ μm yields an imaging condition: $\Phi_{imag}\simeq\frac{2}{3}E_F\simeq 6.7$ meV.

In our experiment the measurement was performed using standard ac technique in a four-terminal configuration. Current was driven at a constant voltage between the emitter and the drain contacts and a voltage was measured between the various voltage probes as a function of V_{GL}. A widely used approach for discussing transport in systems smaller than the phase coherence length is the one due to Landauer.[7,8] A particularly powerful tool within that framework is Büttiker's multiport formula[9]

$$\frac{h}{2e^2}I_\alpha=\tau_\alpha V_\alpha-\sum_{\substack{\beta\\ \beta\neq\alpha}}T_{\beta\alpha}V_\beta, \tag{3}$$

where I_α is the current in the αth probe, $\tau_\alpha=\sum_{\beta\neq\alpha}T_{\beta\alpha}$, $T_{\beta\alpha}$ is the transmission from the βth to the αth probe, and all voltages are measured relative to the drain. By changing the voltage applied to the various gates, the resistances of the three probes and the emitter were tuned to the same value (approximately 1.5 KΩ). Since $I_{P1}=I_{P2}=I_{P3}=0$, $I_E=-(I_{D1}+I_{D2})$, $\tau_{P1}\simeq\tau_{P2}\simeq\tau_{P3}$, and $\tau_P\gg T_{P1P2}$, $T_{P2,P1}$, we obtain for $V_{21}=V_{P2}-V_{P1}$

$$V_{21}\simeq V_E\frac{T_{EP2}-T_{EP1}}{\tau_P}, \tag{4}$$

where $\tau_P=\tau_{P1}=\tau_{P2}=\tau_{P3}$. Since τ_P depends only weakly on the lens potential (the lens potential affects weakly the probes openings), measurement of V_{21} amounts to a direct probing of the difference between the transmission coefficients from the emitter to the two voltage probes $P1$ and $P2$. The focusing by the lens should be reflected then in a maximum in V_{21} as the imaging condition given in Eq. (2) is approached.

In all experiments presented below $V_E=30$ μV (rms) and $\tau_P=h/2e^2\times\frac{1}{1500}\,\Omega^{-1}\simeq 8.6$ leading to the simple relation $T_{EP2}-T_{EP1}=8.6V_{21}/30$ μV. The measured difference in the transmission coefficients, $T_{EP2}-T_{EP1}$, for three different temperatures, is shown in Fig. 3 as a function of the lens gate voltage V_{GL} (similar results are observed for $T_{EP2}-T_{EP3}$). Consider the $T=4.2$ K case first. For $V_{GL}=0$, $T_{EP2}-T_{EP1}$ is already positive, reflecting the partial collimation[2,3] of an electron beam in-

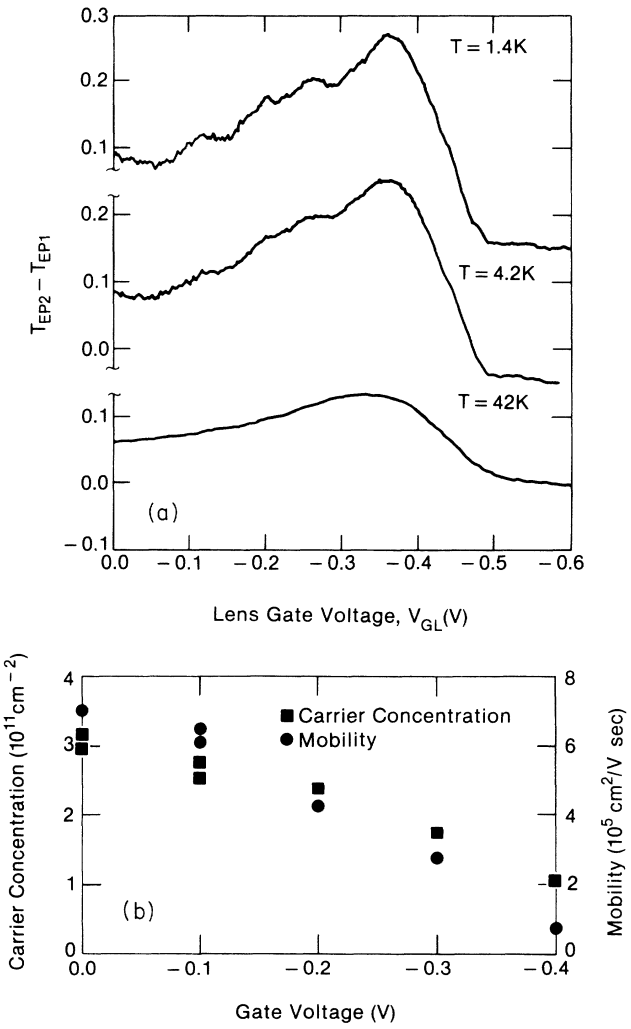

FIG. 3. (a) The difference between the transmission coefficients to the two voltage probes $P1$ and $P2$ vs the voltage applied to the lens gate. The three curves correspond to different temperatures. Focusing condition is satisfied for $V_{GL}=-0.37$ V. (b) Carrier concentration and mobility in a macroscopic gated 2D EG structure as a function of the voltage applied to the gate.

jected from a constriction. The small value of $T_{EP2} - T_{EP1}$ indicates a rather wide angular distribution, in accordance also with magnetic field results presented below. Upon applying negative voltage to the lens gate, $T_{EP2} - T_{EP1}$ increases monotonically, reaches a sharp maximum at $V_{GL} \simeq -0.37$ V, and thereafter drops down. To estimate the lens gate voltage that corresponds to a given potential Φ, we have measured the carrier concentration versus gate voltage in a macroscopic, gated van der Pauw pattern. The results are shown in Fig. 3(b). Substituting the various parameters taken from Fig. 3(b) into Eq. (2) yields for the imaging condition $V_{GL} \simeq -0.38$ V, in good agreement with the peak position in Fig. 3.

At a lower temperature, $T = 1.4$ K, a pronounced, reproducible structure appears superimposed on the focusing curve. The overall focusing effect does not change since the transport mfp is practically independent of temperature. At a temperature $T = 42$ K, however, the curve is smooth and the total focusing effect is considerably smaller [Fig. 3(a)]. At $T \simeq 77$ K (not shown), when the transport mfp becomes roughly 1.2 μm, the focusing signal vanishes altogether, unambiguously proving the ballistic nature of the effect. Notice that the fine structure, superimposed on the focusing signal, disappears at considerably lower temperatures than the focusing peak does. This issue will be briefly addressed later.

A number of undesirable effects tend to decrease the lens efficiency. First, electrons traversing under the lens gate suffer, due to reduced screening, enhanced scattering from the ionized donors in the $Al_xGa_{1-x}As$, especially when Φ approaches E_F. This fact is also evidenced from the degradation in the mobility seen in Fig. 3(b). This effect contributes to the sharp drop in $T_{EP2} - T_{EP1}$ for $|V_{GL}| > 0.4$ V. Second, electrons impinging on the lens potential at a large incidence angle, $\theta_1 > \sin^{-1}(1 - \Phi/E_F)$ [see Fig. 1(b)], are totally reflected. As a consequence of these effects, the focusing peak expected in V_{P2} (relative to a drain in a three terminal measurement) is reduced by the monotonic decrease in the signal as Φ approaches E_F. Measuring V_{21} normalizes out most of these effects and the signal due to focusing is clearly seen. Larger devices with 4 and 6 μm separation between the emitter and voltage probes, a larger lens radius, $R = 600$ nm, and a narrower waist width, $W = 150$ nm, were also fabricated (on a different 2D EG with $N_S \simeq 4 \times 10^{-11}$ cm^{-2} and $\mu \simeq 1 \times 10^6$ cm^2/V sec). As expected from Eq. (2), the peak in $T_{EP2} - T_{EP1}$ was shifted to lower lens gate voltage, $V_{GL} \simeq -0.2$ V (smaller potential Φ), and a clear peak in V_{P2} as a function of V_{GL} had been observed[10] (not shown here). The focusing peak in the latter devices were smaller due to the limited mfp.

To verify further the ballistic nature of the effect, a magnetic field was applied perpendicular to the plane of the 2D EG. The measured difference in the transmission coefficients, $T_{EP2} - T_{EP1}$ vs V_{GL}, for various magnetic fields, is depicted in Fig. 4. We find that the focusing peak decreases as the magnetic field increases and vanishes for fields around $B \simeq 700$ G, where the cyclotron orbit diameter, D_C, becomes comparable to the separation between the emitter and the voltage probes [$D_C = 2(2mE_F)^{1/2}/eB \simeq 2.5$ μm]. The observed sensitivity to

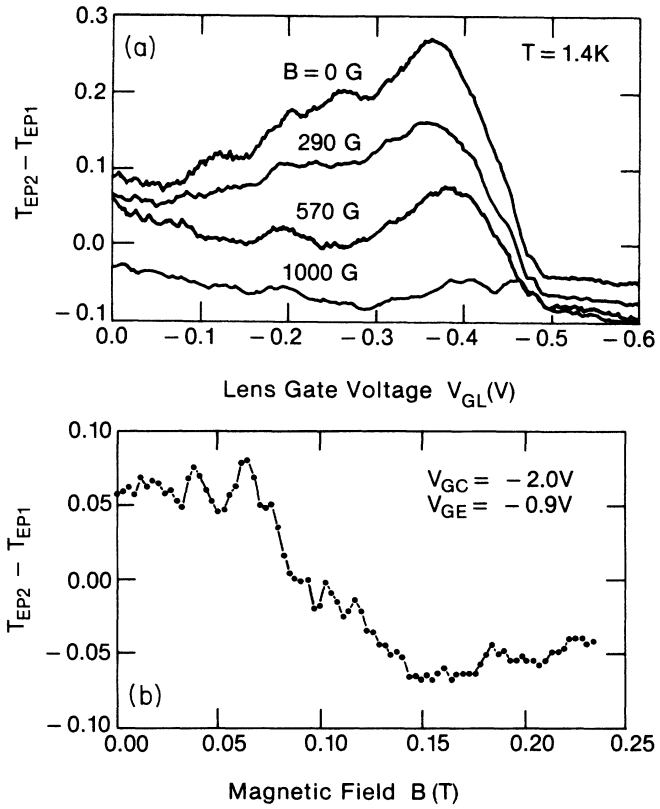

FIG. 4. The difference between the transmission coefficients to the two probes, $P1$ and $P2$ (a) vs the voltage applied to the lens gate for various values of a magnetic field perpendicular to the plane of the 2D EG and (b) vs a magnetic field (for $V_{GL} = 0$). Notice the quantum structure superimposed on the classical behavior. Similar structure is seen in Fig. 3(a) as a function of V_{GL} at $T = 1.4$ K.

weak magnetic fields is indicative of ballistic transport (in contrast to diffusive motion). Complementary data are shown in Fig. 4(b), where $T_{EP2} - T_{EP1}$ is depicted versus magnetic field for $V_{GL} = 0$ (a magnetic steering experiment). The sign reversal observed in the measured V_{21} results from the deflection of the collimated ballistic electrons from $P2$ to $P1$ by the magnetic field. The size of the cyclotron diameter that corresponds to the sign reversal is $D_C \simeq 2.5$ μm, indicating a wide angular distribution. Notice the reproducible structure superimposed on the classical steering curve.

We return now to discuss the reproducible fluctuations in $T_{EP2} - T_{EP1}$ vs V_{GL} and B seen at low temperatures. Usually, the disappearance of quantum fluctuations at temperatures as high as 4.2 K is attributed to thermal averaging. However, for transport on length scales shorter than the elastic mean free path (compared with diffusive motion), the important paths available for the electron are of approximately the same length. The positions of the maxima and minima in the interference pattern would thus depend very weakly on energy, reducing thermal smearing considerably. In the absence of any collisions it is a straightforward matter to show that in our experiment, thermal smearing is approximately an order of magnitude too small to account for the observed disap-

pearance of the quantum fluctuations with temperature.

We therefore suggest that the smearing of the quantum fluctuations might be due to electron-electron scattering. Noticing that both electrons involved in the scattering process should have energies within k_BT from E_F before and after the scattering, it can be shown that in the limit $k_BT \ll E_F$ the scattering must be either forward directed or resulting in an approximate exchange between the electrons momenta. Thus, electron-electron scattering at low temperatures do not affect the classical trajectories, the transport mfp, and the focusing signal, but will randomize the phase of the electrons and therefore will smear a structure due to interference effects. It is evident from the data that the critical temperature for these fluctuations is much lower than the characteristic temperature for which the classical effects (collimation, focusing, etc.) disappear, hence suggesting that they are related to quantum interference phenomena.

Though these fluctuations are similar to the usual conductance fluctuations in the diffusive regime we emphasize that both the distance between the emitter and the voltage probes and the distance between the voltage probes are shorter than the transport mfp. Another possible source for quantum fluctuations in the ballistic regime might be electron diffraction by the constrictions. In the presence of a weak magnetic field the kinetic phase of each semiclassical path from a slit of width $2d$ to a screen at a distance $L \gg d$ is modified by the phase due to the magnetic field. The equiphase planes in the absence of magnetic field are rotated due to the field and the whole diffraction pattern is shifted by $\Delta x = BeL^2/2p$ where p is the electron momentum. Notice that Δx is a classical quantity resulting in a rigid shift of the whole diffraction pattern. The characteristic field scale for shifting one maximum of the diffraction pattern on the screen to the next one is given by $\Delta B = \Phi_0/Ld$. In our experiment, for $2d = 400$ nm we find $\Delta B \simeq 100$ G, which is not inconsistent with the experimental results shown in Fig. 4(b). We emphasize that this curve does not correspond to an ideal diffraction pattern possibly due to scattering. However, the main features of our analysis should remain valid as long as the mfp is much longer than L.

In summary, we have demonstrated the first operation of an electrostatic electron lens in solid-state systems. The focusing is achieved by a spatial modulation of the electrostatic potential in regions where ballistic electrons travel in analogy with refraction of photons in optics. Ballistic motion was confirmed both by monitoring the magnitude of the focusing effect as the temperature is varied and by application of a perpendicular magnetic field.

We thank Y. Imry, A. Palevski, and A. Yacobi for useful discussions and A. Hartstein and N. Albert for their help. One of us (U.S.) was partially supported by the Weizmann foundation.

[1]H. van Houten, B. J. van Wees, J. E. Mooij, C. W. J. Beenakker, J. G. Williamson, and C. T. Foxon, Europhys. Lett. **5**, 721 (1988).

[2]L. W. Molenkamp, A. A. M. Staring, C. W. J. Beenakker, R. Eppenga, C. E. Timmering, J. G. Williamson, C. J. P. M. Harmans, and C. T. Foxon, Phy. Rev. B **41**, 1274 (1990).

[3]U. Sivan, A. Palevski, M. Heiblum, and C. P. Umbach, Proceedings of the Sixth International Conference on Hot Carriers in Semiconductors, 1989 (unpublished).

[4]L. I. Glazman, G. B. Lesovik, D. E. Khmel'nitskii, and R. I. Shekhter, Pis'ma Zh. Eksp. Teor. Fiz. **48**, 218 (1988) [JETP Lett. **48**, 238 (1988)]; N. D. Lang, A. Yacoby, and Y. Imry, Phys. Rev. Lett. **63**, 1499 (1989).

[5]B. J. van Wees, L. P. Kouwenhoven, C. J. J. M. Harmans, T. G. Williamson, C. E. Timmering, M. E. I. Broekaart, C. T. Foxon, and J. J. Harris, Phys. Rev. Lett. **62**, 2523 (1989).

[6]C. G. Smith, M. Pepper, H. Ahmed, J. E. F. Frost, D. J. Hasko, R. Newbury, D. C. Peacock, D. A. Ritchie, and G. A. C. Jones, in Proceedings of the Fourth International Conference on Modulated Semiconductor Structures, Ann Arbor, Michigan, 1989 (unpublished).

[7]R. Landauer, IBM J. Res. Dev. **1**, 223 (1957); R. Landauer, Philos. Mag. **21**, 863 (1970).

[8]Y. Imry, in *Directions in Condensed Matter Physics,* edited by G. Grinstein and G. Mazenko (World Scientific, Singapore, 1986).

[9]M. Müttiker, Phys. Rev. Lett. **57**, 1761 (1986).

[10]An additional test consisted of a similar 2.2 μm device with the lens gate being replaced by a rectangular-shaped gate. As expected, no focusing effect was observed.

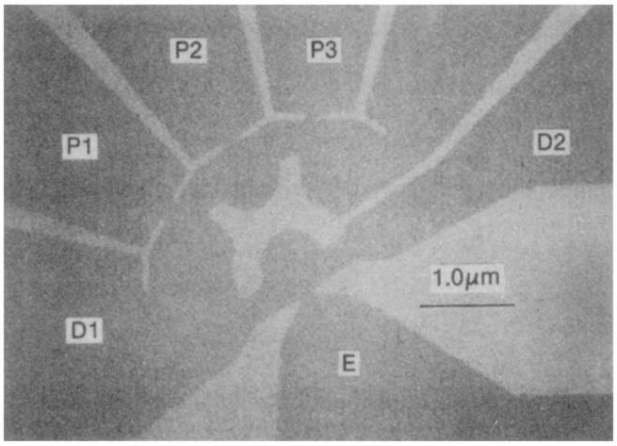

FIG. 2. Scanning electron microscope micrograph of the device (top view). The light areas are the metallic gates forming the emitter, probes, and the biconcave lens, by the induction of potential barriers underneath.